*Radiol Oncol 2006; 40(4): 259-71.*

# Cysteine cathepsins, stefins and extracellular matrix degradation during invasion of transformed human breast cell lines

**Irena Zajc, Aleš Bervar, Tamara T. Lah**

*Department of Genetic Toxicology and Cancer Biology, National Institute of Biology, Ljubljana, Slovenia*

***Background.*** *Human breast cellular model, comprising four cell lines originating from spontaneously immortalized human breast epithelial MCF10A cell line, its c-Ha-ras transfectant, MCF10AT, and two tumourigenic derivatives, cultured from two sequential mouse xenographs, MCF10AT-Ca1a and MCF10AT-Ca1d, were used to compare the relative protein concentration of cathepsins and stefins in single cells.*

***Methods.*** *The relative protein concentration of cathepsins and stefins in single cells was analysed by confocal microscopy, and compared to their protein expression in cell homogenates.*

***Results.*** *The most invasive, MCF10AT cell line contained several fold higher protein concentration of cathepsin B and increased levels of stefins, but similar levels of cathepsin L, compared with the parental MCF10A cells. This was associated with five fold higher endocytosis of Matrigel-DQ-collagen IV (DQC) and a simultaneous increase in signal overlap between DQC and cathepsin L as well as DQC and stefin B, but a decrease in that of DQC and cathepsin B overlap in the MCF10AT cells. Simultaneously, increased signal overlaps between both cathepsins and between cathepsins-stefins pairs, were observed in this cell line.*

***Conclusions.*** *These results suggest that the increased collagen endocytosis and degradation in the invasive phenotype significantly affect also the subcellular localization of cysteine cathepsins and stefins. Based on these and the reports of other authors, we hypothesize that the intracellular degradation may also be associated with cathepsin L, whereas cathepsin B in the ras transformed breast cells is involved in both, the intracellular and pericellular degradation of extracellular matrix during cell migration and invasion.*

*Key words: breast neoplasms; tumor cells, cultured; neoplasms invasiveness; cathepsins; extracellular matrix*

## Introduction

Human genome is known to contain 11 related, but distinct cysteine proteases belonging to papain family C1A, cathepsins (Cats) B, L, H, S, K, F, V, X, W, O and C.[1] Early studies of CatB and CatL have shown

Received 9 October 2006

Accepted 29. November 2006

Correspondence to: Tamara T. Lah, Ph. D., Department of Genetic Toxicology and Cancer Biology, National Institute of Biology, Večna pot 111, 1000 Ljubljana, Slovenia; Phone: +386 1 423 5017; Fax: +386 1 423 5038; E-mail: Tamara.Lah@nib.si ; http://www.nib.si

their wide tissue distribution. They are mostly localized to lysosomes, where they can reach up to 1 mM concentration.[2] In the tumour cell models, the increased secretion of the pro-enzyme and the mature enzyme forms of CatB[3,4] and CatL[5] after the oncogenic transformation has been reported. Besides other proteases, CatB[6] and CatL[7] can directly degrade components of the extracellular matrix, although under slightly different conditions. It has been shown that CatL activation may be accelerated by certain ECM components[8], such as proteoclycans.[9] Cathepsins may also be involved in the proteolytic cascade[10], in which they activate other proteases. In breast carcinoma, altered expression of lysosomal CatB and CatD and altered subcellular trafficking were initially demonstrated by Sameni *et al.*[11] and later confirmed by these and other authors (reviewed in[12]). The interest in the mechanisms of CatB and CatL regulation and activation increased when several clinical studies have shown elevated mRNA, protein and activity levels of CatB and CatL in malignant breast tumour tissues and demonstrated their potential for the prognosis of the disease.[13-16] The activities of cysteine cathepsins are regulated by their endogenous inhibitors, a large superfamily of cystatins. The stefins (St) family comprise the intracellular inhibitors, of which StA and StB were also found to be altered in tumours and sera of cancer patients.[17-20] The structural features of inhibitors and their tight complexes with cathepsins were revisited by Turk and Gunčar.[21] Presumably, their cytosolic location should guard the subcellular structures from the accidental release of active lysosomal cysteine cathepsins, but their intracellular interactions with their target proteases are still not well understood.

To establish whether CatB and CatL are associated with an invasive cell phenotype and with the ability to form tumours after the injection at a secondary site (tumourigenicity), we have used a cell model of four breast cell lines, originating from parental MCF10A cell, which is described in details in Materials and methods below. In this model, we found that the *in vitro* invasiveness did not correlate with cell ability to form malignant tumours in mice, the most invasive cell line being the MCF10AT and selective synthetic inhibitors of CatB and CatL impaired the *in vitro* invasion of these cells.[22] In the present study, we focus on the expression and the localization of CatB and CatL and their inhibitors StA and StB in the transformed breast cells during the invasion through Matrigel-collagen matrix. The aims of this study were: (a) to determine the relative abundance of cathepsins and stefins in different breast cells during their invasion into Matrigel-collagen matrix using confocal microscopy in comparison with their expression levels in cell homogenates, (b) to develop the software tools for faster, cost-effective, automatic and more objective single-cell image stack analysis, including analysis of signal overlapping of different antigens and (c) to examine the overlapping signals of cathepsins and stefins inside the tumour cells, along with the degraded endocytosed collagen type IV (DQ-collagen IV) in the parental MCF10A, and invasive MCF10AT cell lines.

## Materials and methods

### *Cell lines*

We used a model of four epithelial breast cell lines derived from spontaneously immortalized cells of a fibrocystic breast patient. The parental cell line was the immortalized diploid cell line MCF10A.[23] The MCF10AT line is MCF10A transfected with c-Ha-*ras* oncogene[24,25] and has an acquired ability to grow in immunodeficient mice. MCF10AT-Ca1a and MCF10AT-Ca1d, obtained by

multiple passages of MCF10AT cells in nude mice, are fully malignant. MCF10AT-Ca1a cells mostly produce undifferentiated carcinoma and MCF10AT-Ca1d cells form heterogeneous carcinomas.[26] These lines were originated at Barbara Ann Karamanos Cancer Institute (Detroit), and kindly provided by Prof. Bonnie Sloane, Department of Pharmacology, WSU, Detroit MI, USA. Cell lines were grown as described previously.[22]

*Preparation of cell lysates and enzyme-linked immunosorbent assay (ELISA)*

The cells were scraped and pelleted by centrifugation at 150g for 5min. They were homogenized by sequential freezing in liquid nitrogen and thawing at 37ºC (3 X) in 50mM Tris buffer, pH 6.9, containing 0.05% (v/v) Brij 35, 0.5mM DTT (dithiothreitol), 5mM EDTA, 0.5mM PMSF (paramethylsulphonyl fluoride) and 10mM pepstatin A. The lysates were centrifuged at 12,000g for 15min and the supernatants stored at –20°C.

ELISA kits for human CatB, CatL, StA and StB were obtained from Krka d.d., Slovenia and performed as suggested by the manufacturer. Purified human CatB, CatL, StA and StB were used as the standards. For CatB, rabbit polyclonal anti-CatB antibodies (IgG) and sheep anti-CatB antibodies (horseradish peroxidase-conjugated) were used as the capture and detection antibodies, respectively. For CatL, polyclonal sheep anti-CatL, for StA, monoclonal mouse anti-StA, and for StB, monoclonal mouse anti-StB antibodies were used as the capture and the detection antibodies. Total protein concentrations were determined using Bradford assay (Bio-Rad, USA). Mean values of at least three independent measurements and standard errors of the mean (SEM) were calculated. Statistical significance was determined with t-test and $p < 0.05$ was considered significant.

*Confocal microscopy*

Each of 8 wells on a Chamber Slide™ (Lab Tec®, Nunc Inc., USA) was pre-coated with 150 μl of fibronectin (16.7 μg/ml, 2.5 μg per well, Sigma) and coated with 200 μl of Matrigel (1 mg/ml, Becton Dickinson, USA), with added 0.2%, or 1% fluorescently labelled DQ-collagen IV, DQC (Molecular Probes, USA). 200,000 cells in 100 μl of medium were seeded and grown for another 24 h. Then the cells were washed with PBS and fixed with 200 μl of 3.7% formaldehyde for 30 min at 37 C in 5% $CO_2$. After washing with PBS, cells were permeabilized for 5 min with 150 μl of 0.2% Triton X-100 (Sigma). Polyclonal and monoclonal antibodies were tested with comparable intensity of labelling and herein mouse clones of the primary antibodies for cathepsins and stefins were used (all by Krka d.d., Slovenia) at 2 mg/ml final concentration. Secondary antibodies, excited at various wavelengths, AlexaFlour 488 rabbit anti-mouse IgG, AlexaFlour 546 goat anti-mouse IgG, and AlexaFlour 633 rabbit anti-mouse IgG, were then applied according to the instructions of the supplier (Molecular Probes, USA). Samples were imaged using laser scanning confocal microscope Leica TCS SP2 at the three channels with excitation wavelengths 488 nm, 546 nm and 633 nm. Images were recorded at 1000× enlargement in series of fifty to eighty 512×512 pixel images (size of a pixel in x and y directions app. 50-300 nm) at 150-1000 nm distance in the z-axis. Each cell (cell group), *e.g.* each stack of images, was then analyzed with Image software (available on the internet and developed by Wayne Rasband, wayne@codon.nih.gov). Software analysis, customised plug-ins, were developed in our laboratory specifically for this purpose. Due to the space limitations these plug-ins are not explained in detail but are available upon request.

The first plug-in was developed to detect edges of the cells. The selected regions of

interest were then transformed by another plug-in into a mask, used to separate possible multiple cells. These masks were then used for quantification, with pixels outside the mask taken as zero signals. The algorithm applied to the mask calculates the volume of the cell (in actual units, e.g. $\mu m^3$), absolute and average values of the signal in each of the three channels (488 nm, 546 nm and 633 nm) and allows signal-overlap measurements of the three channels using a specifically derived formula.[27] Another plug-in detects background (noise) structures of non-specific shape and deletes them. Although some noise still has to be omitted manually by checking each slice, our method is much faster, and more precise than manual selection of cell edges.

Overlapping signals are the closest this method can get to actually monitor the antigens' subcellular co-localizations. As the size of the cell in pixels (radius between about 50 and 200 pixels) is not large enough for precise separation and localization of the organelles, the signal overlap relates to the localization of the antigens to the same area of the cell, but not to the co-localization to the same subcellular organelle. This signal-overlap was determined by calculating "overlap index" for each pixel of the image (500 × 500 × 50-80 pixels). The index was calculated for each pair of the channels separately (488 nm – 546 nm, 488 nm – 633 nm, 546 nm – 633 nm). The index took into account the relative signal intensity (0-256) of each pixel compared to the background of the individual slice (generally between 10 and 20). These relative intensities were therefore generally larger than one but not higher than about 20. Finally, relative signal intensities of the two signals (e.g. at 488 nm and 546 nm) were multiplied so that only in the cases where signals in both pixels were strong, the index could reach high enough values to be taken into consideration for calculation. The average overlap index across the cell and at the wavelength pairs was calculated by the appropriate statistical analyses, using up to 50 single-cell measurements for each category, *e.g.* images with different combinations of labelled Cats B and L, Sts A and B and degraded DQC, respectively.[27]

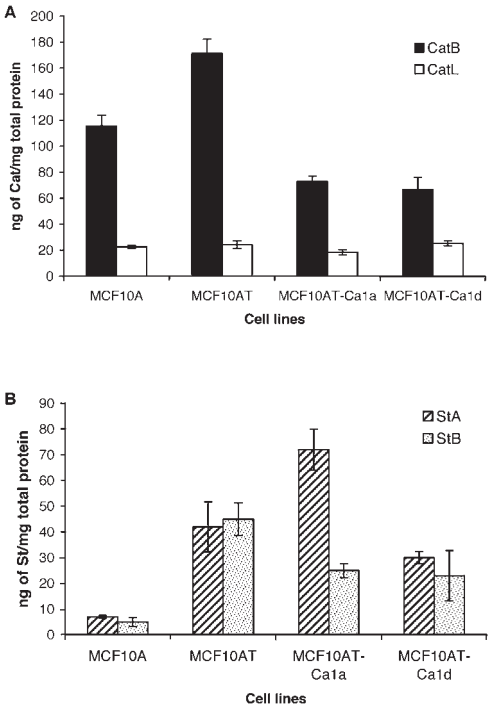


**Figure 1.** *Protein expression of CatB and CatL, StA and StB in the lysates of human breast epithelial cell lines, MCF10A, MCF10AT, MCF10AT-Ca1a and MCF10AT-Ca1d.*
Cells were grown on Matrigel, homogenized and protein expressions of cathepsins and stefins were determined by ELISAs as described in Materials and methods. Mean values from three independent experiments are presented. Error bars depict SEM. The statistical significance was determined by t-test and $p < 0.05$ was considered significant. The cell lines are listed according to their increased tumourigenicity.
**(a)** CatB protein concentration was the highest in MCF10AT cells ($p = 0.003$) and significantly lower in MCF10AT-Ca1a ($p = 0.002$) and MCF10AT-Ca1d cell lines ($p = 0.004$), compared to MCF10A cells. CatL expression was similar in all four cell lines.
**(b)** StA and StB were both significantly increased in MCF10AT, MCF10AT-Ca1a, and MCF10AT-Ca1d cells (all $p<0.005$) compared to the parental line.

## Results

### *Cathepsins and stefins protein expression in cell cultures by ELISA*

As previously demonstrated, the MCF10AT, obtained after *ras* transfection of the parental MCF10A cell line, was the most invasive, whereas the two cell lines, MCF10AT-Ca1a and MCF10AT-Ca1d, which were obtained from xenographts of the MCF10AT cell line, although having higher tumourigenicity than the parental cell line, are less invasive in *in vitro* Matrigel assays.[22-27] CatB protein expression was the highest in MCF10AT ($p = 0.003$), and significantly lower in MCF10AT-Ca1a ($p = 0.002$) and MCF10AT-Ca1d cell lines ($p = 0.004$), compared to MCF10A cells (Figure 1a). CatL expressions were similar in all four cell lines.

StA and StB were both significantly increased in MCF10AT, MCF10AT-Ca1a, and MCF10AT-Ca1d cells (all $p<0.005$) compared to the parental line (Figure 1b). Noteworthy, StB expression was the highest in MCF10AT, similar as was that of CatB. The relative expression of these antigens was similar as observed previously,[22] when these cells were grown on the plastic surface, although on the Matrigel, all protein levels are about two fold lower compared to the plastic surface. Noteworthy, the molar ratios calculations (between cathepsins and stefins) showed that there was about 60-90 fold overexpression of cathepsins in MCF10A, and slightly decreased in the malignant cells lines.

### *Analysis of cathepsins, stefins and the Matrigel-collagen by confocal microscopy*

A representative example of immunohistochemical labelling in a model of the four lines is shown on Figure 2. The quantitative fluorescence analysis of single cell images by confocal microscopy parallels the data in cell lysates. Quantification of CatB in MCF10A and MCF10AT cells by confocal microscopy showed its significantly higher expression in the MCF10AT than in the parental cells. The increased pericellular distribution of CatB was observed in MCF10AT, confirming the previous findings.[11,28] In MCF10AT-Ca1a and MCF10AT-Ca1d cells, spreading of CatB immunostaining over the whole cell was observed. CatL distribution was not significantly changed in these cells compared to MCF10A cells. The expression of stefins was markedly elevated, particularly in tumourigenic cell lines, compared to MCF10A cells.

The last panel represents degraded DQC (green) in the four cell lines, grown on Matrigel, enriched with DQC. Slight, pericellular degradation of DQC was observed in the parental cells. In contrast, the intracellular degradation of DQC in MCF10AT was about 5-times higher than in MCF10A cells and both, extracellular and pericellular degradation of DQC was observed. The intracellular degradation of DQC was also abundant in the tumourigenic cells in spite of the fact that the latter are less invasive *in vitro.*[22] Taken together, these results show that the parental cell line contained the least of endocytosed matrix, least dispersion of cathepsins staining and low levels of both stefins.

### *Subcellular distribution and co-localization of antigens*

The 3-D analysis was performed on a sample size a few hundred single cells. These were imaged in over 100 stacks of 50-80 slices with the size of 512 × 512 pixels at three different wavelengths of the excitation laser, as described in Material and methods. For reasons of clarity, we will present the process of the confocal image analysis using one slice of a single stack. Figure 3a presents a raw image of the MCF10AT cell labelled with DQC (488nm channel – left),

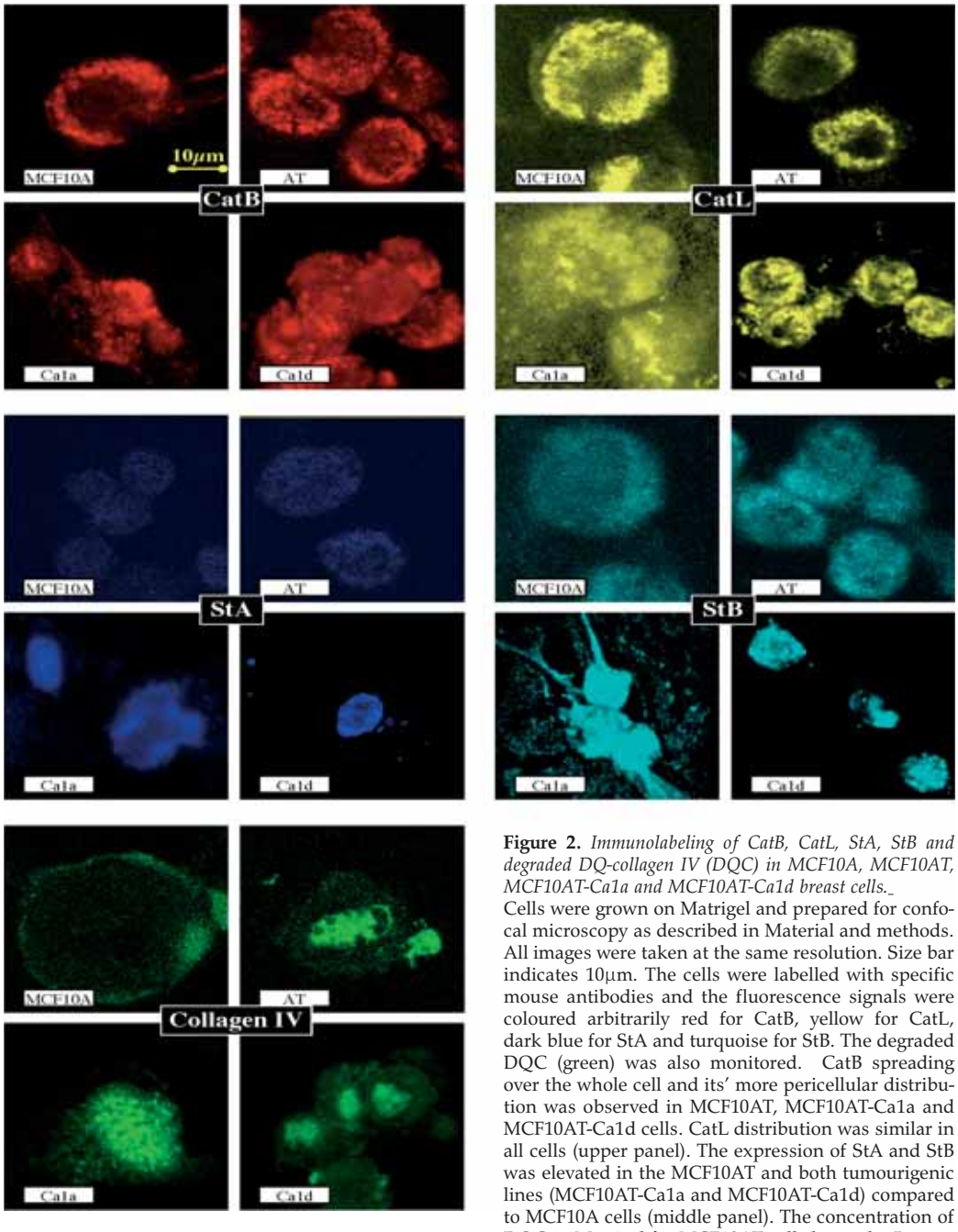


**Figure 2.** *Immunolabeling of CatB, CatL, StA, StB and degraded DQ-collagen IV (DQC) in MCF10A, MCF10AT, MCF10AT-Ca1a and MCF10AT-Ca1d breast cells.*
Cells were grown on Matrigel and prepared for confocal microscopy as described in Material and methods. All images were taken at the same resolution. Size bar indicates 10μm. The cells were labelled with specific mouse antibodies and the fluorescence signals were coloured arbitrarily red for CatB, yellow for CatL, dark blue for StA and turquoise for StB. The degraded DQC (green) was also monitored. CatB spreading over the whole cell and its' more pericellular distribution was observed in MCF10AT, MCF10AT-Ca1a and MCF10AT-Ca1d cells. CatL distribution was similar in all cells (upper panel). The expression of StA and StB was elevated in the MCF10AT and both tumourigenic lines (MCF10AT-Ca1a and MCF10AT-Ca1d) compared to MCF10A cells (middle panel). The concentration of DQC in Matrigel for MCF10AT cells has to be 5-times lower than in other cell lines, otherwise the signal was too strong for imaging. Intracellularly degraded DQC was expressed at a higher level in MCF10AT, MCF10AT-Ca1a and MCF10AT-Ca1d cells compared to the parental cells.

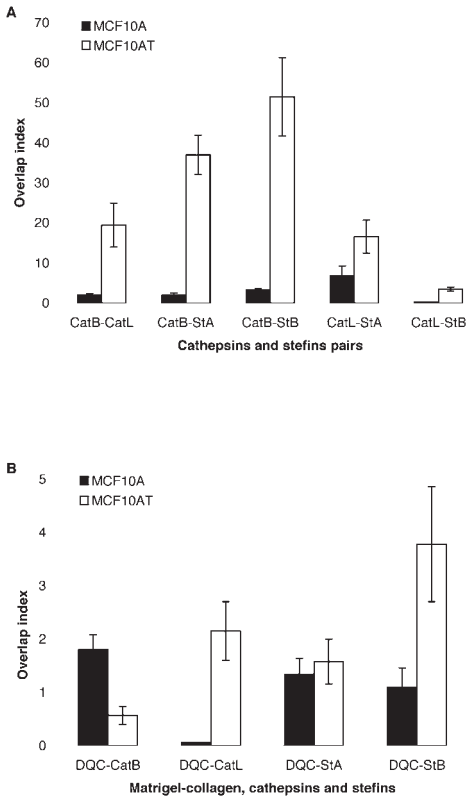


**Figure 4.** *Signal-overlap of cathepsins, stefins and DQ-collagen in MCF10A and MCF10AT cells.*
The overlap index was calculated as described in Materials and methods. Error bars depict SEM. Note the different scales of panels A and B. **(a)** Overlap indexes between cathepsins and stefins were measured in all pairs. The signal overlap was higher in MCF10AT cells than in the MCF10A cells. This increase in the signal overlap was highly significant between CatB and both stefins, and between CatL and StB ($p = 0.0001$), less so between CatB and CatL ($p = 0.0065$), and barely significant between CatL and StA ($p = 0.049$). In invasive MCF10AT cells, CatB-CatL overlapping was relatively low compared with the overlap indexes between CatB and stefins. **(b)** Overlap indexes between DQC and CatB, CatL, StA, and StB showed a significant increase in the signal overlap observed in MCF10AT compared to MCF10A cells between DQC and CatL ($p = 0.0002$) and DQC and StB ($p = 0.0155$). In contrast, the overlap index between DQC and CatB was significantly lower ($p = 0.0018$) in MCF10AT cells. That between DQC and StA was similar in both cell lines.

the antibodies against CatL (546nm – middle) and the antibodies against StB (633nm – right). To these raw images we applied the first and most extensive plug-in, that used an algorithm designed to detect whether or not there is a significant gradient of signal strength, which dubbed an edge at each individual point. The plug-in also detected the angle at which this edge was going through the pixel in question. To achieve this, a roster of 9 × 9 pixels surrounding the pixel in question was analysed. If adjacent pixels had edges running in the same direction (angles not differing by more than a preset number, e.g. 5° or 10°), an edge was drawn on the resulting image (Figure 3b). In Figure 3c, the results of the second plug-in are shown. It was designed to check for the size and shape of the resulting closed shapes and to fill the shapes that were meeting the criteria of size and circularity. The next plug-in (Figure 3d) combined all three channels into one (Figure 3d middle). The red line was manually drawn after reviewing single slices (Figure 3d left) and comparing it to a composite image throughout the depth of all 55 slices (Figure 3d right).

Figure 4a shows the signal overlap between both cathepsins and between cathepsins and stefins. In MCF10AT cells, CatB overlapped better with either of the stefins than CatL did. Consistently a higher signal overlap observed in MCF10AT cells than in the paternal MCF10A cells, may be also due to the increased immunostaining of both cathepsins and stefins in the former cell line. Figure 4b presents the signal overlap indexes between the degraded DQC (Matrigel) and cathepsins and stefins in the invasive MCF10AT compared with the benign parental cell line. A significant increase in the signal overlap was observed in MCF10AT compared to MCF10A cells between DQC and CatL ($p = 0.0002$) and DQC and StB ($p = 0.0155$). In contrast, the

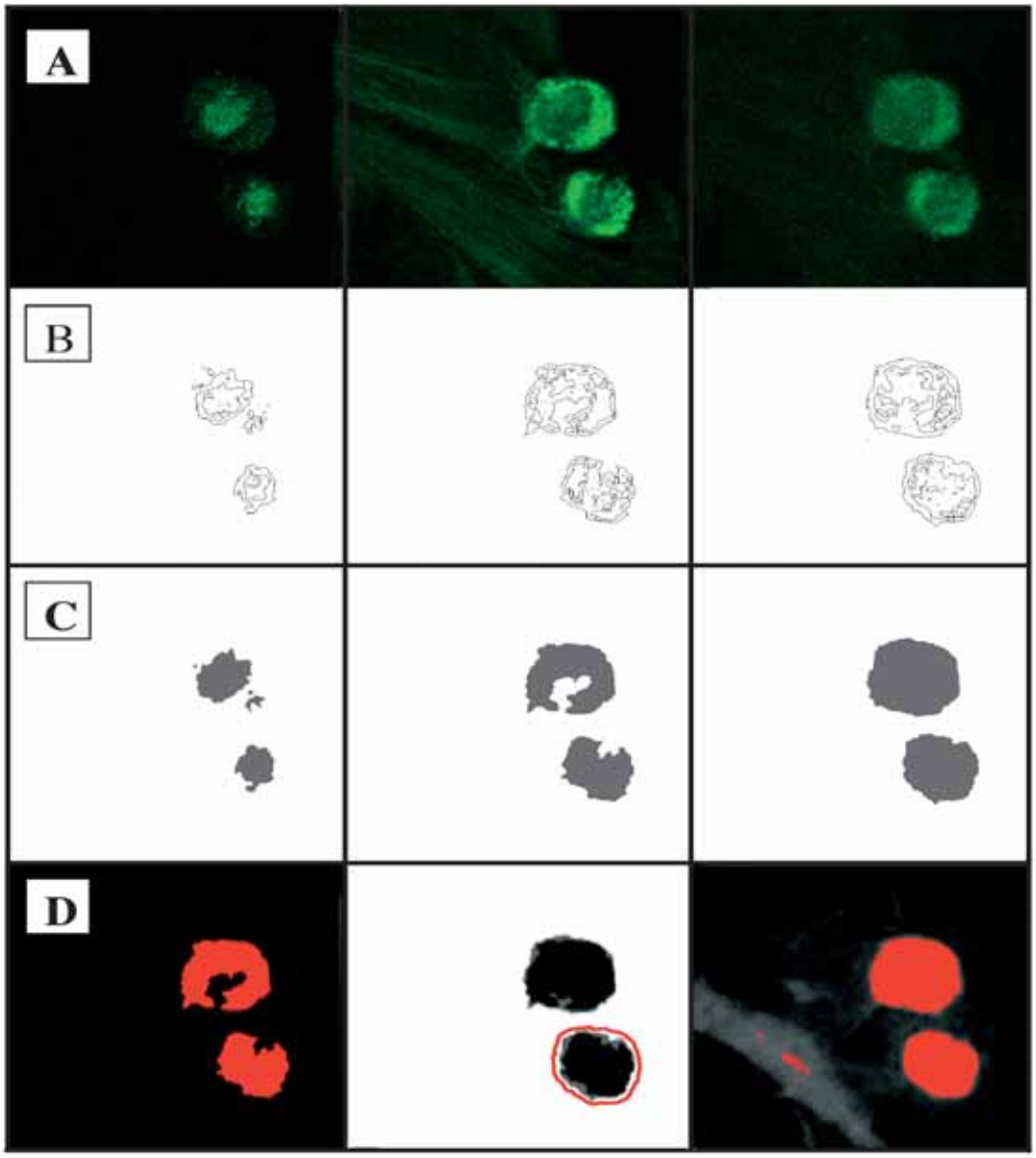


**Figure 3.** *The development of software tools for the quantitative image analysis of confocal images.*
A single slice of a MCF10AT cell is presented**.** The software plug-ins are described in Materials and methods. The stack of images can be browsed using a slide bar on the bottom to view any slice of the stack at any chosen time. **(a)** The un-edited images of a single slice of MCF10AT cell at three different wavelengths: left – 488nm, DQ-collagen IV; middle – 546nm, CatL, right – 633nm StB, as derived from the confocal microscope. The green color was chosen arbitrarily. **(b)** The same slice after the plug-in for edge detection. The plug-in automatically detects cell borders and intracellular margins based on the changes in the intensity of the signal that meet predefined criteria. **(c)** The slice after the plug-in that fills the encircled areas and removes the areas that are too small or do not meet the defined shape criteria. The removing process can be best observed when panels (b) and (c) of the left image are compared. **(d)** Final (manual) processing of the slice. Left: The three areas calculated in (c) were merged into one that represents the total area of interest in the slice. Middle: The area representing a single cell was selected manually (red line). Right: The view through the whole stack (50-80 slices) allowed the easier overview of the cell size and position. Some structures shown on this view clearly do not represent cells and these were removed by the plug-ins.

overlap index between DQC and CatB was significantly lower ($p = 0.0018$) in MCF10AT cells. That between DQC and StA was similar in both cell lines. Similarly, the overlap index between the DQC and StB was significantly increased in MCF10AT cells, whereas that of stefin A was similar as in MCF10A cells.

## Discussion

The present work is the continuation of the study on lysosomal cathepsins and their inhibitors in a panel of four human breast epithelial cell lines, which represents a cellular model for the development of malignant phenotypes.[22] We examined the expression of cysteine cathepsins and their inhibitors at protein levels in cell lysates on one hand, and on the other hand by confocal microscopic imaging, which may give an alternative insight into the proteolysis associated with the invasion into collagen matrix. For the latter we developed a novel software programme for the partially automatic analysis of confocal images by using multiple imaging channels to monitor and quantitate the proteins along with the degradation of DQC. Imaging data confirmed the measurements in cell lysates, showing increased levels of CatB, but not CatL protein in the most invasive, *ras* transfected cells. CatB was lower in the two less invasive, but more tumourigenic cell lines and in the paternal cells, whereas CatL expression was similar in all four cell lines. These results indicated that the *ras* transfection of the breast epithelial cells affected specifically CatB expression and mostly its trafficking,[11,28] but not that of CatL. This is different as recently reported by Collette *et al*. for mouse fibroblasts and rat ovarian epithelial cells, where *ras* signalling pathways resulted in markedly up-regulated CatL, but not CatB.[5] The authors also emphasized that *ras* signalling is cell type specific and may affect lysosomal cathepsins in different ways. Indeed, in our transformed breast cells, CatL and CatB were differentially affected by the *ras* oncogene transfection and were obviously independently regulated. A functional role for *ras* in cathepsin B trafficking and redistribution to cell surface has also been observed in melanoma, osteoclasts and human colorectal carcinoma (sumarized in ref [12]), similar as observed in this study. We also reported on the independent regulation of both cathepsins in another panel of breast cancer cell lines[29-31] and same notion was deduced from the clinical studies.[13,15,16,32]

It has been suggested that a misbalance between cathepsins and their inhibitors contributes to the progression of tumors.[16-18] In this study, both stefins were upregulated in the more invasive as well as in the tumourigenic cells. From the calculated molar ratios between individual cathepsins and stefins, being much higher than equimolar, we may conclude that the concentration of these two inhibitors may not be sufficient to inhibit these two cysteine cathepsins. However, in another panel of breast cancer cells lines, obtained from breast cancer patients with different genetic alterations, we found an inverse correlation between the invasiveness and stefins' expression.[30] In this and other studies on expression of stefins in cancer progression, the findings are not conclusive: lower, similar or higher levels of stefins were found in tumour tissue homogenates in the clinical studies of breast and prostate carcinoma,[32,33] suggesting the complex regulation of stefins in tumours progression.

In this study, we observed a partial signal overlap between cathepsins and stefins, indicating that they are to some extent colocalized to the same cellular area, but not necessarily to the same cellular organelles. This supports the data from the first at-

tempt to localize the cathepsins and stefins by confocal microscopy, revealing their differential localization in human embryonic liver and hepatoma cells.[34] Noteworthy, CatB and StB co-localization seems to be the highest in the invasive cells, whereas CatL co-localization with stefins was relatively lower in the invasive cells. This may result in higher CatL efficacy in the intracellular collagen degradation, which certainly also depends on the local access of stefins to bind to CatL.

Collagen turnover is critical to tumour expansion and several previous studies addressed the questions of the subcellular sites of its degradation. Sameni *et al.*[35] showed that collagen degradation was predominantly pericellular in BT20, and mostly intracellular, localized to lysosomes, in BT549, both breast cancer cell lines. They have also demonstrated that proteolysis is pericellular in breast carcinoma spheroids and pericellular, as well as intracellular, in the colon carcinoma spheroids, with the stroma and inflammatory cells contributing to the degradation of collagen.[36] In prostate carcinoma cells, the DQ-collagen I and DQ-collagen IV degradation was reduced by inhibitors of matrix metallo, serine and cysteine proteases,[37] suggesting a complex interplay among these proteases in matrix degradation. In the MCF10A-neoT cells, Premzl *et al.*[28] clearly defined a co-localization of extracellular and intracellular fraction of CatB, presumably responsible for both, the pericellular and intralysosomal DQ-collagen IV degradation, respectively. The authors also reported on the major role of cathepsin B activity in the intracellular substratum degradation during capillary–like tube formation of endothelial cells grown on Matrigel by differential inhibition of Z-Arg-Arg-cresyl violet degradation by the inhibitor CA-074Me and not by the non-methylated form CA-074, under the conditions permisive for cell penetration.[38] However, Montaser *et al.*[39] demonstrated that CA-074Me inactivates both CatB and CatL within living murine fibroblasts, whereas CA-074 is really inhibiting CatB selectively and therefore all previous data do not exclude the involvement of CatL in the substratum degradation. However, to our knowledge, there is no direct evidence for CatL involvement in the intracellular substratum degradation, for example by using highly selective inhibitors and/or selective substrates for CatL that would easily penetrate the living cells.

The intracellular localizations of collagen may be explained by findings of Kjøller *et al.*,[40] who reported that a glycoprotein, urokinase plasminogen activator receptor-associated protein (uPARAP/Endo180) was responsible for import and lysosomal delivery of extracellular collagen IV and that its degradation was impaired in the presence of the cysteine protease inhibitors. Genetic ablation of uPARAP/Endo180 impaired collagen turnover during mammary carcinoma progression.[41] Montcourrier *et al.*[42] found that another lysosomal cathepsins, CatD, is co-localized to and responsible for the degradation of the extracellular matrix in large acidic vesicles in the breast cancer cells, and speculated that increased intracellular substratum degradation is not only assisting tumour cell invasion, but is also important to provide tumour cells with amino acid reservoir, necessary for their the increased metabolic activity and protein synthesis. In line with this hypothesis is our finding that the intracellular degradation of collagen was not only elevated in the invasive cell type, but was actually elevated in all cancer cells lines, compared to the parental cell line, regardless of their invasive potential.

The presented confocal microscopy data are an attempt to quantitate the signal overlap of the key players of the intracellular cysteine dependent proteolysis and their

functions. A high signal overlap of CatL (but not that of CatB) with the intracellularly degraded collagen (despite being present in about five times lower concentrations than CatB) indicates that CatL may be more important for the intracellular degradation of collagen type IV. A high signal overlap index between the stefins and degraded DQC suggests that stefins are in the proximity of the cathepsins-collagen complexes and may affect cathepsins activities. However, to confirm their functionality, *in situ* activity and the co-localization of enzymes and inhibitors, additional experiments by simultaneous organelle-specific labelling are needed.

In conclusion, we were able to show that the semi-quantitative analysis of cellular levels of cathepsins and stefins by confocal images in single cell gives complementary information to the measurements in the cell lysates. Confocal microscopy and the developed software for the single-cell image stack analysis supported the biochemical analysis, demonstrating an increased labelling of CatB, StA and StB in the invasive MCF10AT compared with the parental MCF10A cells, whereas CatL was expressed equally. Much higher levels of endocytosed, degraded DQC in the invasive than in the parental line, and a simultaneous increase in the signal overlap of collagen and CatL, suggests possible involvement of CatL in the intracellular degradation of the substratum, complementary to that of CatB, what has to be confirmed in future experiments.

## Acknowledgments

This study was supported by the Ministry of Higher Education, Science and Technology of the Republic of Slovenia (Programme # 0105-509, T.T Lah) and by 6FP Cancerdegradome, # 503297 (to T.T.Lah, #17). We thank Prof. Dr. Bonnie Sloane for providing us with the cell lines thate have been obtaind via the collaboration on International & Cooperative Projects Foggarty International, NIH, USA,. 1RO3 TW00952-01, 1999-2001.

## References

1. Berdowska I. Cysteine proteases as disease markers. *Clin Chim Acta* 2004; **342:** 41-69.

2. Xing R, Addington AK, Mason RW. Quantification of cathepsins B and L in cells. *Biochem J* 1998; **332:** 499-505.

3. Linebauch BE, Sameni M, Day NA, Sloane BF, Keppler D. Exocytosis of active cathepsin B. *Eur J Biochem* 1999; **264:** 100-9.

4. Frosch BA, Berquin I, Emmert.Buck M, Moin K, Sloane BF. Molecular recognition, membrane association and secretion of tumour cathepsin B. *APMIS* 1999; **107:** 28-37.

5. Collette J, Ulku AS, Der CJ, Jones AS, Erickson AH. Enhanced Cathepsin L expression is mediated by different ras effector pathways in fibroblasts and epithelial cells. *Int J Cancer* 2004; **112:** 190-9.

6. Buck MR, Karustis DG, Day NA, Honn KV, Sloane BF. Degradation of extracellular-matrix proteins by human cathepsin B from normal and tumour tissues. *Biochem J* 1992; **282:** 273-78.

7. Felbor U, Dreier L, Bryant RAR, Ploegh HL, Olsen BR, Mothes W. Secreted cathepsin L generates endostatin from collagen XVIII. *EMBO J* 2000; **19:** 1187-94.

8. Ishidoh K, Kominami E. Procathepsin L degrades extracellular matrix proteins in the presence of glycosaminoglycans in vitro. *Biochem Biophys Res Commun* 1995; **217:** 624-31.

9. Kihara M, Kakegawa H, Matano Y, Murata E, Tsuge H, Kido H, et al. Chondroitin sulfate proteoglycan is a potent enhacer in the processing of procathepsin L. *Biol Chem* 2002; **383:** 1925-29.

10. Schmitt M, Janicke F, Graeff F. Tumour-associated proteinases. *Fibrinolysis* 1992; **6:** 3-26.

11. Sameni M, Elliott E, Ziegler G, Fortgens PH, Dennison C, Sloane BF. Cathepsins B and D are localized at the surface of human breast cancer cells. *Pathol Oncol Res* 1995; **1:** 43-53.

12. Cavallo-Medved D, Sloane BF. Cell surface cathepsin B: Understanding its functional significance. *Curr Top Dev Biol* 2003; **54:** 313-31.

13. Lah TT, Kokalj-Kunovar M, Štrukelj B, Pungerčar J, Barlič-Maganja D, Drobnič-Košorok M, et al. Stefins and lysosomal cathepsins B, L and D in human breast carcinoma. *Int J Cancer* 1992; **50:** 36-44.

14. Foekens JA, Kos J, Peters HA, Krašovec M, Look MP, Cimerman N, et al. Prognostic significance of cathepsins B and L in primary human breast cancer. *J Clin Oncol* 1998; **16:** 1013-21.

15. Thomssen C, Schmitt M, Goretzki L, Oppelt P, Pache L, Dettmar P, et al. Prognostic value of the cysteine proteases cathepsin B and cathepsin L in human breast cancer. *Clin Cancer Res* 1995; **1:** 741-6.

16. Lah TT, Čerček M, Blejec A, Kos J, Gorodetsky E, Somers R, et al. Cathepsin B, a prognostic indicator in lymph node-negative breast carcinoma patients: comparison with cathepsin D, cathepsin L and other clinical indicators. *Clin Cancer Res* 2000; **6:** 578-84.

17. Calkins CC, Sloane BF. Mammalian cysteine protease inhibitors: Biochemical properties and possible roles in tumour progression. *Biol Chem* 1995; **376:** 71-80.

18. Kos J, Lah TT. Cysteine proteinases and their endogenous inhibitors: Target proteins for prognosis, diagnosis and therapy in cancer. *Oncol Rep* 1998; **5:** 1349-61.

19. Kos J, Werle B, Brunner N. Cysteine proteinases and their inhibitorsin extracellualr fluids: Markers for diagnosis and prognosis in cancer. *Int J Biol Markers* 2000; **15:** 84-9.

20. Kos J, Lah TT. Cystatins in cancer. In: Kopitar Jerala N, Žerovnik E, editors. *Human stefins and cystatins, molecular anatomy and physiology of proteins series.* New York: NOVA Science Publishers Inc; 2006.

21. Turk D, Gunčar G. Lysosomal cysteine proteases (cathepsins): promising targets. *Acta Crystallogr* 2003; **D 59:** 203-13.

22. Bervar A, Zajc I, Sever N, Katunuma N, Sloane BF, Lah TT. Invasiveness of transformed human breast epithelial cell lines is related to cathepsin B and inhibited by cysteine proteinase inhibitors. *Biol Chem* 2003; **384:** 447-55.

23. Soule HD, Maloney TM, Wolman SR, Peterson WD Jr, Brenz R, McGrath CM, et al. Isolation and characterization of a spontaneously immortalized human breast epithelial cell line MCF10. *Cancer Res* 1990; **50:** 6075-86.

24. Basolo F, Elliott J, Tait L, Chen XQ, Maloney T, Russo IH, et al. Transformation of human breast epithelial cells by c-Ha-ras oncogene. *Mol Carcinogenesis* 1991; **4:** 25-35.

25. Dawson PJ, Wolman SR, Tait L, Heppner G, Miller FR. MCF10AT: a model for the evolution of cancer from proliferative breast disease. *Am J Pathol* 1996; **148:** 313-9.

26. Santner SJ, Dawson PJ, Tait L, Soule H, Eliason J, Mohamed AN, et al. Malignant MCF10CA1 cell lines derived from premalignant breast epithelial MCF10AT cells. *Breast Cancer Res Treat* 2001; **65:** 101-10.

27. Bervar A. *Localization of cathepsins B and L and their inhibitors, stefins A and B in the invasiveness of breast cancer cell lines.* PhD thesis. Ljubljana: Ljubljana University; 2002.

28. Premzl A, Zavašnik-Bergant V, Turk V, Kos J. Intracellular and extracellular cathepsin B facilitate invasion of MCF-10A neoT cells through reconstituted extracellular matrix in vitro. *Exp Cell Res* 2003; **283:** 206-14.

29. Lah TT, Calaf G, Kalman E, Shinde BG, Russo J, Jarosz D, et al. Cathepsins D, B and L in breast carcinoma and transformed human breast epithelial cells (HBEC). *Biol Chem* 1995; **376:** 357-63.

30. Zajc I, Sever N, Bervar A, Lah TT. Expression of cysteine peptidase cathepsin L and its inhibitors stefins A and B in relation to tumourigenicity of breast cancer cell lines. *Cancer Lett* 2002; **187:** 185-90.

31. Zajc I, Frangež L, Lah TT. Expression of cathepsin B is related to tumourigenicity of breast cancer cell lines. *Radiol Oncol* 2003; **37:** 233-40.

32. Levičar N, Kos J, Blejec A, Golouh R, Vrhovec I, Frkovič-Grazio S, et al. Comparison of potential biological markers cathepsin B, cathepsin L, stefin A and stefin B with urokinase and plasminogen activator inhibitor-1 and clinicopathological data of breast carcinoma patients. *Cancer Det Prev* 2002; **26:** 42-9.

33. Sinha AA, Jamuar MP, Wilson MJ, Rozhin J, Sloane BF. Plasma membrane association of cathepsin B in human prostate cancer: biochemical and immunogold electron microscopic analysis. *Prostate* 2001; **49:** 172-84.

34. Calkins CC, Sameni M, Koblinski J, Sloane BF, Moin K. Differential localization of cysteine protease inhibitors and a target cysteine protease, cathepsin B, by immuno-confocal microscopy. *J Histochem Cytochem* 1998; **46:** 745-51.

35. Sameni M, Moin K, Sloane BF. Imaging proteolysis by living breast cancer cells. *Neoplasia* 2000; **2:** 496-504.

36. Sameni M, Dosescu J, Moir K, Sloane BF. Functional imaging of proteolysis: stromal and inflammatory cells increase tumour proteolysis. *Mol Imaging* 2003; **2:** 1-17.

37. Podgorski I, Linebaugh BE, Sameni M, Jedeszko C, Bhagat S, Cher ML, et al. Bone microenvironment modulates expression and activity of cathepsin B in prostate cancer. *Neoplasia* 2005; **7:** 207-23.

38. Premzl A, Turk V, Kos J. Intracellular proteolytic activity of cathepsin B is associated with capillary-like tube formation by endothelial cells in vitro. *J Cell Biochem* 2006; **97:** 1230- 40.

39. Montaser M, Lalmanach G, Mach L. CA-074, but not its methyl ester CA-074Me is a selective inhibitor of cathepsin B witin living cells. *Biol Chem* 2002; **383:** 1306-8.

40. Kjøller L, Engelholm LH, Høyer-Hansen M, Danø K, Bugge TH, Behrendt N. uPARAP/endo180 directs lysosomal delivery and degradation of collagen IV. *Exp Cell Res* 2004; **293:** 106-16.

41. Curino AC, Engelholm LH, Yamada SS, Holmbeck K, Lund LR, Molinolo AA, et al. Intracellular collagen degradation mediated by uPARAP/Endo180 is a major pathway of extracellular matrix turnover during malignancy. *J Cell Biol* 2005; **169:** 977-85.

42. Montcourrier P, Mangeat PH, Valembois C, Salazar G, Sahuquet A, Duperray C, et al. Characterization of very acidic phagosomes in breast cancer cells and their association with invasion. *J Cell Sci* 1994; **107:** 2381-91.